Spherical Nanoporous $LiCoPO_4$/C Composites as High Performance Cathode Materials for Rechargeable Lithium Batteries

Jun Liu,[§,†] Thomas E. Conry,[§,‡] Xiangyun Song,[†] Li Yang,[†] Marca M. Doeff, [*,‡] and Thomas J. Richardson[*,†]

[†]Environmental Energy Technologies Division, and [‡]Materials Science Division, Lawrence Berkeley National Laboratory, Berkeley, CA 94720 USA.

§Jun Liu and Thomas E. Conry contributed equally to this work. *Corresponding author: Email: TJRichardson@lbl.gov (T.J.R.); MMDoeff@lbl.gov (M.M.D).

KEYWORDS Lithium-ion batteries, energy storage, $LiCoPO_4$, nanoporous, spray-pyrolysis.

Spherical nanoporous $LiCoPO_4$/C composite microparticles were synthesized from soluble precursors by spray pyrolysis. They consisted of ~70 nm primary particles agglomerated into micron-sized spheres with an average pore size of 68 nm and a 3 - 5 nm thick conformal carbon coating comprising 2.4 % carbon by weight. The material delivered a reversible capacity of 123 mAh/g at C/10 rate, and showed excellent cycling behavior and rate capability. The good electrochemical performance is due to the presence of three-dimensional networks for both electronic and ionic transport.

One way to achieve higher energy densities in Li ion batteries is to incorporate cathodes having significantly higher redox potentials. This approach is particularly attractive for electric vehicle applications[1-3] because fewer high voltage cells are needed in the 300V packs used as power sources for the vehicles. The assembly of the packs is simplified, less hardware is required (further increasing the system specific energy) and cost is lowered. Examples of high voltage cathodes under consideration are $Li_2FeMn_3O_8$ and $LiMn_{1.5}Ni_{0.5}O_4$ 5 V spinels,[4-6] and $LiMPO_4$ (M = Co, Ni) olivines.[7-10] Among these, $LiCoPO_4$ is appealing since it offers both a flat high potential (~4.8 V vs. Li/Li^+) and good theoretical capacity (167 mAh/g).[7] Electrolyte degradation due to the high working potential, however, along with a 7% unit cell volume change during charge and discharge, contribute to poor cycling performance. [11] Low intrinsic ionic and electronic conductivities also may adversely impact the rate capability and utilization of $LiCoPO_4$.[12]

Nanoengineering techniques have been successfully implemented to improve the electrochemical performance of olivine-type $LiFePO_4$ and, to a lesser extent, $LiMnPO_4$. These include: decreasing particle sizes to the nanoscale, thereby minimizing electron and Li^+ diffusion distances within the solid phase;[13-15] modifying the particle surfaces with nanometer thick conductive coatings to improve the electronic conductivity;[16-19] and creating nanoporous microstructures to facilitate the Li^+ charge-transfer kinetics at the solid/liquid interface between the active material and electrolyte.[20-22] Few such efforts, however, have been directed toward $LiCoPO_4$.[23, 24]

Although nanostructuring is expected to improve the electrochemical performance of $LiCoPO_4$, very small particles often do not pack well and can be difficult to process into composite electrodes, resulting in lower practical energy densities. In contrast, micron-sized spherical particles pack well and are easy to process into electrodes.[25,26] The ideal $LiCoPO_4$ electrode material would consist of large spherical agglomerates of nanosized primary particles. Here we describe the preparation of micron-sized nanoporous spherical $LiCoPO_4$/C particles using a simple and scalable spray pyrolysis method.[27,28]

The spray-pyrolysis setup has been described previously.[29] To make $LiCoPO_4$, $Co(CH_3CO_2)_2{\cdot}4H_2O$, $LiNO_3$, $NH_4H_2PO_4$ and citric acid ($HOC(COOH)(CH_2COOH)_2$) in a 1:1:1:0.5 molar ratio were dissolved in de-ionized water to form a solution in which the concentration of Co^{2+} was 0.5 mol/L. This solution was delivered via syringe pump to an atomizer nozzle (Sonozap Model 120K50ST, 120 kHz) to generate microdroplets, which were transported through a preheated quartz tube (700 °C) by a carrier gas (5% H_2 + 95% N_2). The product collected at the end of the tube was further heat-treated at 700 °C in N_2 for 3 h to improve the conductivity of the carbon coating.

Cathodes were prepared by mixing 85 wt % $LiCoPO_4$/C with 10 wt % carbon black and 5 wt % polytetrafluoroethylene binder, rolling the mixture into thin sheets, and cutting into circular electrodes of 1.26 cm^2 area. The electrodes typically had an active material loading of 4-5 mg. Coin cells assembled with composite cathodes, metallic lithium anodes, 1M $LiPF_6$ in 1:1 (v/v) diethyl carbonate/ethylene carbonate electrolyte with 1 wt.% LiBOB (lithium bis(oxalato) borate) additive (employed to stabilize the interface between cathode material and electrolyte), and Celgard 2500 polypropylene separators were cycled between 3 and 5 V.

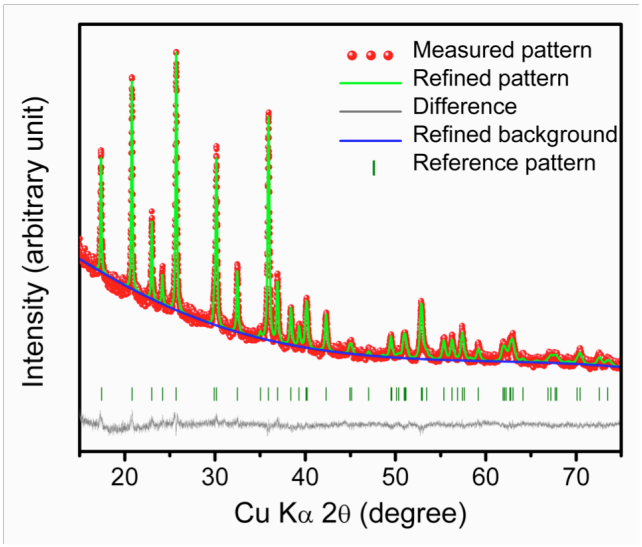

Figure 1. XRD pattern of the nanoporous $LiCoPO_4$/C composite material with refined pattern.

The formation mechanism for $LiCoPO_4$/C microspheres made by spray pyrolysis is shown schematically in Figure S1. A fine aerosol of aqueous precursor droplets was sprayed into the hot zone of a tube furnace, where the fast evaporation of water and reaction of the precursors created porous spheres of nanocrystalline $LiCoPO_4$. The decomposition of organic components formed a conductive carbon coating on the $LiCoPO_4$ crystallites, and the gas evolution from the reactions created three dimensionally interconnected nanopores in the spherical secondary particles. The XRD pattern of the composite and its Rietveld refinement are shown in Figure 1. All diffraction peaks were indexed in the *Pnma* space group with a = 10.1997 Å, b = 5.9209 Å, c = 4.7002 Å, and V = 283.85 $Å^3$ (R_{wp}=4.82%), in agreement with reported values.[7] The results of site-occupancy refinement suggested the presence of few defects. The average primary particle size, determined from peak broadening, was about 70 nm.

The spherical $LiCoPO_4$/C composite particles had diameters ranging from a few to 15 μm for most particles (Fig. 2a, b). Figure 2b shows the surface of an individual particle with numerous open pores. Some of the spheres were hollow (Fig. 2c), while others were filled (Fig. 2d).

Hierarchically organized pores extend throughout the secondary particles, allowing the liquid electrolyte to penetrate into their interiors. EDS elemental mappings (Figs. 2e-g) show a uniform distribution of Co, P, O and C, consistent with the $LiCoPO_4$ phase purity determined by XRD. $LiCoPO_4$/C particles, purposely fractured by mechanical grinding, were characterized by TEM. Figures 3a and 3b show the numerous pores with sizes ranging from a few nanometers to a few hundred nanometers, surrounded by nano-sized $LiCoPO_4$ crystallites. HRTEM images of the edge (Fig. 3c) and interior (Fig. 3d) of a nanopore reveal an amorphous 3-5 nm thick carbon layer on all surfaces.

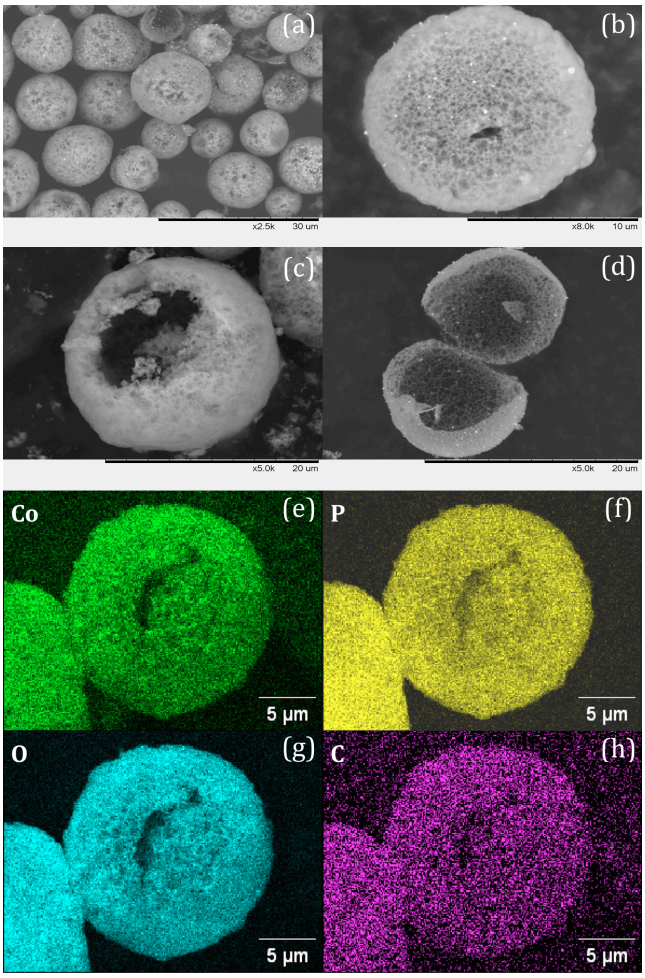

Figure 2. SEM images of (a) the nanoporous $LiCoPO_4$/C composite particles; (b) the surface of a single particle; (c, d) broken particles, showing the 3D interconnected pores; EDS maps of (e) Co, (f) P, (g) O, and (h) C for a single $LiCoPO_4$/C particle.

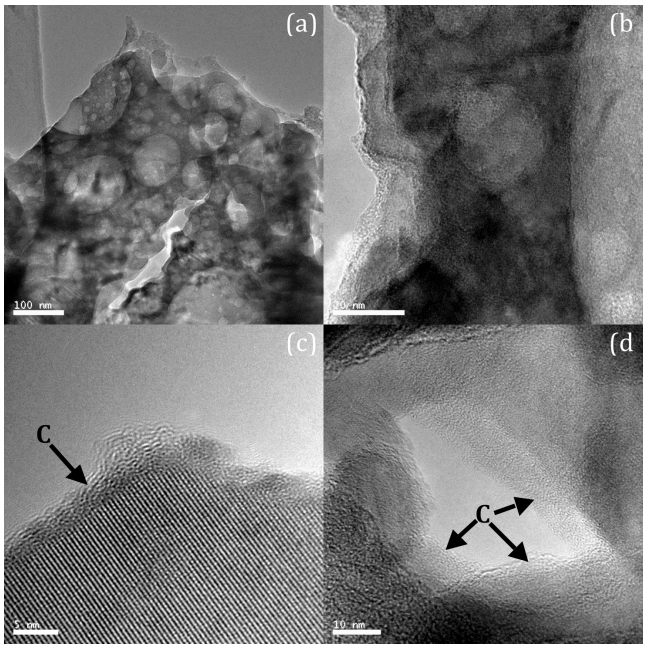

Figure 3. (a) TEM image of a fractured $LiCoPO_4$/C particle, showing the pore structure; (b) TEM image showing the nanocrystalline character of the composites; (c, d) HRTEM images of the fracture edge and the inside of a nanopore, the amorphous carbon coating on both the outer surface and the inner pore walls.

The carbon content of the $LiCoPO_4$/C composite was determined by TGA (Fig. S2a). A weight loss of 2.4% was recorded for the composite, while that for uncoated $LiCoPO_4$ was negligible. XRD patterns (Fig. S2b) measured before and after heating were identical, indicating that the change in weight is entirely due to combustion of carbon.

N_2 adsorption/desorption isotherms, shown in Figure S3, were used to determine the Brunauer-Emmett-Teller (BET) surface area and the average pore size. The type IV curve with a large H3 hysteresis loop is consistent with N_2 adsorption in a nanoporous solid.[30] The loop closes abruptly at $P/P^\circ = 0.42$, corresponding to the emptying of pores with small apertures into the intergranular void space. The BET surface area and average pore size were found to be 76 $m^2\ g^{-1}$ and 68 nm, respectively.

The electrochemical performance of the nanoporous $LiCoPO_4$/C in lithium half-cell configurations is summarized in Figure 4. In contrast to the behavior of isostructural $LiFePO_4$ and $LiMnPO_4$,[13,15] which both have a single, flat voltage plateau, two voltage plateaus were observed in both charge and discharge (Fig. 4a) . These have been associated with two first-order phase transitions corresponding to $LiCoPO_4$ $Li_{0.7}CoPO_4$ and $Li_{0.7}CoPO_4$ $CoPO_4$.[12,31] The observed coulombic inefficiency is most likely due to side reactions involving the electrolyte.[12]

A discharge capacity of 123 mAh/g was obtained at C/10 (Fig. 4a, inset), where C/X corresponds to the current necessary to fully discharge (charge) the battery in X hours. $LiCoPO_4$ cathodes have generally suffered from poor cycling stability.[32] In contrast, the nanoporous $LiCoPO_4$/C composite exhibited a capacity retention of 95% over 20 cycles. This may be attributable to the stabilization effect introduced by the LiBOB additive,[33] and/or to the presence of the conformal carbon coating. The coulombic efficiency steadily increased from 86% for the 1st cycle to 97%, consistent with a protective effect developing from the products of an irreversible reaction during early cycles, akin to the solid electrolyte interface (SEI) that forms on graphite anodes.

Discharge profiles at various C-rates are shown in Figure 4b. Even when discharged at 5C, a capacity as high as 82 mAh g^{-1} was achieved, indicating that the nanostructuring strategy employed in this study resulted in superior rate capability.

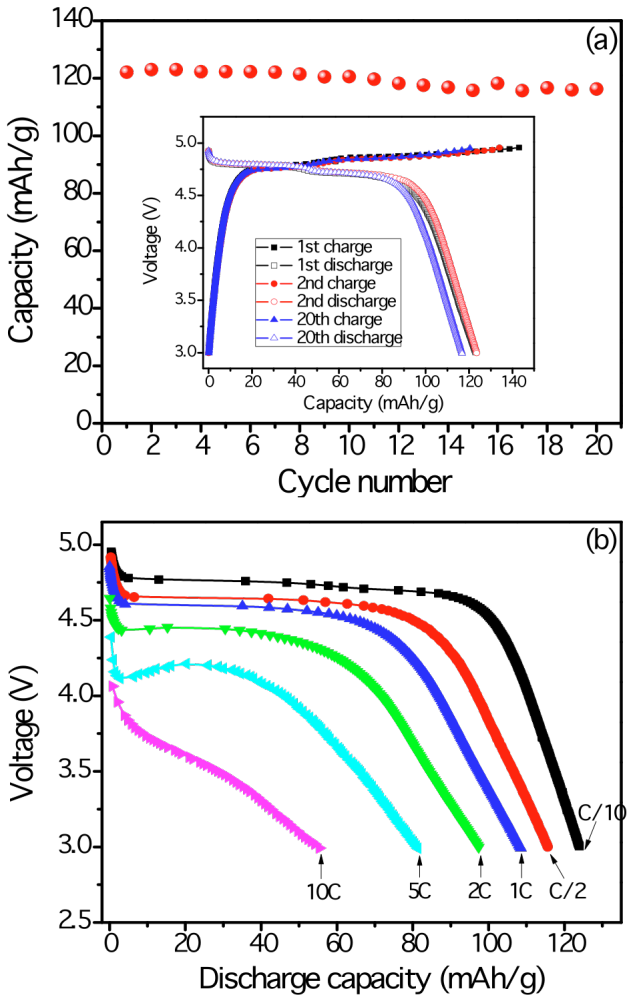

Figure 4. (a) Charge-discharge profiles at C/10, (inset) capacity retention and coulombic efficiency at C/10; (b) Discharge profiles at varying rates.

These results suggests that the spray pyrolysis method used to prepare the spherical nanoporous $LiCoPO_4$/C composite may usefully be applied to other candidate electrode materials with intrinsically slow kinetics, such as $LiMPO_4$, Li_2MSiO_4, and $LiMBO_3$ (M = Fe, Mn, Co), to improve their power capabilities through engineering of primary particle and pore sizes, secondary particle sizes and shapes, and surface coatings for improved conductivity and resistance to degradation.

Nanoporous microspheres consisting of ~70 nm sized carbon coated $LiCoPO_4$ primary particles were prepared by spray pyrolysis from aqueous precursor solutions. The $LiCoPO_4$/C composites were employed as cathode materials in lithium half-cells. These cells exhibited excellent rate capability, with over 80 mAh/g delivered at a 5C rate, and 123 mAh/g at C/10. The capacity retention upon cycling at C/10 rate was 95% after the twentieth discharge, with coulombic efficiencies of 97% after the first cycle. These good electrochemical characteristics are attributed to the microstructure of the composites, which allow facile electronic and ionic transport.

Acknowledgement. This work was supported by the Assistant Secretary for Energy Efficiency and Renewable Energy, Office of Vehicle Technologies of the U.S. Department of Energy under contract no. DE-AC02-05CH11231. The authors would like to thank HydroQuebec for a gift of $LiCoPO_4$.

Supporting Information Available: Detailed experimental procedures and material synthesis schematic, TGA and additional XRD analysis, N_2 adsorption/desorption isotherms.

(1) Armand, M.; Tarascon, J.-M. *Nature* **2008**, *451*, 652.
(2) Manthiram, A.; Murugan, A. V.; Sarkar, A.; Muraliganth, T. *Energy Environ. Sci.* **2008**, *1*, 621.
(3) Goodenough, J. B.; Kim, Y. *Chem. Mater.* **2010**, *22*, 587.
(4) Kawai H.; Nagata M.; Tabuchi M.; Tukamoto H.; West A.R. *Chem. Mater.* **1998**, *10*, 3266. (5) Liu, J.; Manthiram, A. *Chem. Mater.* **2009**, *21*, 1695.
(6) Liu, J.; Manthiram, A. *J. Phys. Chem. C* **2009**, *113*, 15073.
(7) Amine, A.; Yasuda, H.; Yamachi, M. *Electrochem. Solid State Lett.* **2000**, *3*, 178.
(8) Bramnik, N. N.; Bramnik, K. G.; Buhrmester, T.; Baehtz, C.; Ehrenberg, H.; Fuess, H. *J. Solid State Eletrochem.* **2004**, *8*, 558.
(9) Murugan, A. V.; Muraliganth, T.; Ferreira, P. J.; Manthiram A. *Inorg. Chem.* **2009**, *48*, 946.
(10) Wang, F.; Yang, J.; NuLi, Y.; Wang, J. *J. Power Sources* **2010**, *195*, 6884.
(11) Bramnik, N. N.; Nikolowski, K.; Baehtz, C.; Bramnik, K. G.; Ehrenberg, H. *Chem. Mater.* **2007**, *19*, 908.
(12) J.-M. Tarascon, M. Armand, *Nature* **2001**, *414*, 359.
(13) Murugan, A. V.; Muraliganth, T.; Manthiram A. *Electrochem. Comm.* **2008**, *10*, 903.
(14) Kang, B.; Ceder, G. *Nature* **2009**, *458*, 190.
(15) Choi, D.; Wang, D.-H.; Bae, I.-T.; Xiao, J.; Nie, Z.; Wang, W.; Viswanathan, V. V.; Lee,Y. J.; Zhang, J.-G.; Graff, G. L.; Yang, Z.-G.; Liu, J. *Nano Lett.* **2010**, *10*, 2799.
(16) Ravet, N.; Chouinard, Y.; Magnan, J. F.; Besner, S.; Gauthier, M.; Armand, M. *J. Power Sources* **2001**, *97-98*, 503.
(17) Herle, P. S.; Ellis, B.; Coombs, N.; Nazar, L. F. *Nature Mater.* **2004**, *3*, 147.
(18) Huang, Y. H.; Goodenough, J. B. *Chem. Mater.* **2008**, *20*, 7237.
(19) Wilcox, J. D.; Doeff, M. M.; Marcinek, M.; Kostecki, R. *J. Electrochem. Soc.* **2007**, *154*, A389.
(20) Dominko, R.; Bele, M.; Goupil, J. M.; Gaberscek, M.; Remskar, M.; Hanzel, D.; Arcon, I.; Jamnik, J. *Chem. Mater.* **2007**, *19*, 2960.
(21) Doherty, C. M.; Caruso, R. A.; Smarsly, B. M.; Drummond, C. J. *Chem. Mater.* **2009**, *21*, 2895.
(22) Liu, J.; Kunz, M.; Chen, K.; Tamura, N.; Richardson, T. J. *J. Phys. Chem. L* **2010**, *1*, 2120.
(23) Shui, J. L.; Yu, Y.; Yang, X. F.; Chen, C. H. *Electrochem. Comm.* **2006**, *8*, 1087.
(24) Li, H. H.; Jin, J.; Wei, J. P.; Zhou, Z.; Yan, J. *Electrochem. Comm.* **2009**, *11*, 95.
(25) Qian, J.; Zhou, M.; Cao, Y.; Ai, X.; Yang, H. *J. Phys. Chem. C* **2010**, *114*, 3477.
(26) Oh, S. W.; Myung, S.-T.; Oh, S.-M.; Oh, K. H.; Amine, K.; Scrosati, B.; Sun, Y.-K. *Adv. Mater.* **2010**, *22*, 4842.
(27) Konstantinov, K.; Bewlay, S.; Wang, G. X.; Lindsay, M.; Wang, J. Z.; Liu, H. K.; Dou, S. X.; Ahn, J. H. *Electrochimica Acta* **2004**, *50*, 421.
(28) Yang, M.; Teng, T.; Wu, S. *J. Power Sources* **2006**, *159*, 307.
(29) Liu, J.; Conry, T. E.; Song, X.; Doeff, M. M.; Richardson, T. J.; *Energy Environ. Sci.* **2011**, *under review*.
(30) Gregg, S. J.; Sing, K. S. W. *Adsorption, Surface Area, and Porosity, 2nd ed.*; Academic Press: New York, 1982.
(31) Nakayama, M.; Goto, S.; Uchimoto, Y.; Wakihara, M.; Kitayama, Y. *Chem. Mater.* **2004**, *16*, 3399.
(32) Wolfenstine, J. *J. Power Sources* **2006**, *158*, 1431.
(33) Liu, J.; Chen, Z.; Busking, S.; Amine, K. *Electrochem. Comm.* **2007**, *9*, 475.from Oxford Press.

SYNOPSIS TOC Nanoporous, micron-sized spherical particles allow for easier processing of Li-ion battery electrodes, without compromising energy density or power capability. This work describes the approach with $LiCoPO_4$, a high-voltage cathode material, synthesized via spray-pyrolysis. Excellent electrochemical performance and stability is achieved.

Authors are required to submit a graphic entry for the Table of Contents (TOC) that, in conjunction with the manuscript title, should give the reader a representative idea of one of the following: A key structure, reaction, equation, concept, or theorem, etc., that is discussed in the manuscript. The TOC graphic may be ***no wider than 7.0 cm*** and ***no taller than 3.5 cm***. The graphic will be reproduced at 100% of the submission size. A surrounding margin will be added to this width and height during *Journal* production.

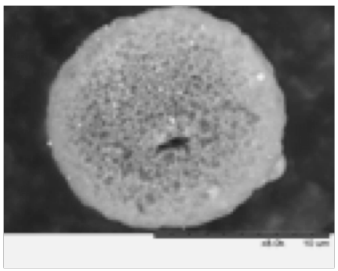

DISCLAIMER